ELSEVIER

Physica D 107 (1997) 383–391

PHYSICA D

Interaction potentials and inherent structures in liquids, glasses, and crystals

Frank H. Stillinger [1]

Lucent Technologies Inc., Murray Hill, NJ 07974, USA

Abstract

A representation in terms of inherent structures (potential minima) and their basins of attraction provides a convenient means for analyzing condensed-phase equilibrium and irreversible processes. In particular this approach is natural for investigating implications of the potential energy "rugged landscape" for glass formation, and its general features lead to formulation of a hypercube model for the collection of inherent structures and their dynamical transitions. A specific realization of this hypercube model exhibits a first-order melting/freezing transition as well as supercooled and superheated metastable states; it also illustrates how artificial Kauzmann temperatures (ideal glass transitions) can seem to arise from limited-range thermodynamic properties. Lists of open mathematical and chemical problems generated by the inherent structure approach terminate the presentation.

Keywords: Glasses; Hypercube; Inherent structures; Supercooling; Superheating

1. Introduction

The particles that form condensed phases experience strong and unremitting interactions with their neighbors. The many-particle potential energy function Φ that comprises all of these interactions controls crystal structure, determines thermodynamic properties and phase transitions, and underlies all kinetic properties. Materials vary widely in each of these attributes owing primarily to chemical distinctions that influence the respective Φ functions. The present paper examines several aspects of the way that the multidimensional "rugged landscape" presented by Φ connects to measurable properties, particularly those observed for supercooled liquids and glasses.

Section 2 reviews general features of realistic Φ's, and discusses the Φ hypersurface in the multidimensional configuration space of all particle coordinates; in particular the steepest-descent map generates a natural division of the space into "basins of attraction." Section 3 extends the geometric characterization of the rugged Φ landscape by invoking the "inherent structure" representation [1–3]. In order to simplify the extremely challenging geometric problem that is generally involved, Sections 4 and 5 present a hypercube model for Φ basins and their kinetic interconnections. This model facilitates discussion and understanding of liquid supercooling and glass transitions, and is particularly useful for analyzing the striking phenomena displayed by fragile glass formers [4,5]. Finally, Section 6 is devoted to

[1] Corresponding author. Tel.: 908-582-4500; fax: 908-582-3958; e-mail: fhs@bell-labs.com.

PII S0167-2789(97)00106-1

a listing of open problems generated by the inherent structure viewpoint, and by its hypercube-model embodiment.

2. Potentials and their basins

Suppose that a large number N of molecules forming a condensed phase of interest reside within volume V. Each molecule i possesses a center position, orientation, and conformation (if any) that are specified by vector $\mathbf{r}_i (1 \leq i \leq N)$. The interaction potential for this collection of molecules, $\Phi(\mathbf{r}_1 \cdots \mathbf{r}_N)$, represents the Born–Oppenheimer ground-electronic-state energy for the system, with origin chosen so that Φ vanishes for widely separated molecules.

The function Φ contains chemical information about the molecules involved including size, shape, flexibility, multipole moments, and polarizability. It includes dispersion attractions, and for many important glass-forming liquids the capacity to engage in hydrogen bonding. Selected cases may also involve breakage and reformation of covalent chemical bonds. But leaving chemical distinctions aside, Φ generally will exhibit the following mathematical properties: (i) invariance under permutation of identical particles; (ii) continuity and differentiability away from nuclear confluences; and (iii) thermodynamic stability arising from a lower bound of the form

$$\Phi > -BN, \tag{2.1}$$

where B is positive and N-independent.

Assuming that each molecule possesses ν internal degrees of freedom, the configuration space spanned by $\mathbf{r}_1 \cdots \mathbf{r}_N$ will have dimension $(\nu+3)N$. This space contains an enormous array of local Φ minima, each representing a mechanically stable arrangement of the molecules in 3-space, an "inherent structure". General considerations [1] establish that in the large system limit the number of local Φ minima Ω grows asymptotically as follows:

$$\Omega \sim N! \exp(\alpha N), \quad \alpha > 0. \tag{2.2}$$

Each minimum belongs to an equivalence class of $N!$ that differ only by particle permutations, while the number of essentially distinguishable minima rises exponentially with N (at fixed N/V).

The full multidimensional configuration space can be naturally and exhaustively divided into "basins", one surrounding each Φ local minimum. These are defined to be the loci of configuration space points all of which connect to the same minimum by means of steepest descent on the Φ hypersurface [1,2,6]. Transition states (simple saddle points) reside at the boundary shared by a pair of contiguous basins, and it is through the neighborhood of these transition states that interbasin dynamical transitions can be expected to occur.

In addition to the asymptotic enumeration property, Eq. (2.2), the basins and the local Φ minima that they surround present the following general characteristics [2].

(A) Elementary transitions between contiguous basins involve localized particle rearrangements and are seldom purely permutational. The corresponding potential energy change measured by the respective Φ minima is just O(1) as a consequence.

(B) The span of Φ minima (difference between the absolute minimum and the highest-lying relative minimum) is $O(N)$. Owing to (A) above, these extremes must be widely separated in the configuration space.

(C) The boundary of each basin contains $O(N)$ transition states. As a result, the positive temperature transition rate also is $O(N)$, i.e. the mean residence time in a basin is $O(N^{-1})$.

(D) Transition state barriers can be arbitrarily low in the dominant portion of configuration space that is characterized by amorphous Φ minima. These low barriers create the quantized two-level degrees of freedom that appear to be a universal property of low-temperature glasses [7,8].

The description just given is appropriate for constant volume conditions. In the event that, instead, constant pressure conditions apply, pV should be added to the intermolecular interactions, and V treated as an additional coordinate [3,9].

3. Inherent structure representation

Let ϕ stand for basin depth on a per-particle basis i.e. the value of Φ/N at the embedded inherent structure minimum. This intensive order parameter offers a natural way to distinguish and to classify the huge collection of basins presented by a macroscopic condensed-phase system. Under this classification scheme, the density in ϕ of inherent structures has a form asymptotically consistent with Eq. (2.2) above,

$$N! \exp[\sigma(\phi)N], \quad \sigma(\phi) \geq 0. \tag{3.1}$$

For the subset of basins with depth parameter ϕ, the intrabasin vibrational free energy per particle may be denoted by $f_v(\beta, \phi)$. Here β is $(k_B T)^{-1}$, and the formal definition of f_v includes intrabasin anharmonic effects to all orders [1,3,9].

The definitions of σ and f_v lead to a simple variational expression for F, the free energy of the N-body system, that is an exact identity in the large-N limit [1,2,6]:

$$\beta F(\beta)/N = \min_{(\phi)}\{\beta\phi - \sigma(\phi) + \beta f_v(\beta, \phi)\} + K(\beta) \tag{3.2}$$

$K(\beta)$ is an additive contribution determined only by the properties of a single molecule, and has no relevance for the remainder of this paper. The variational minimum indicated in Eq. (3.2) will be attained at a temperature-dependent depth $\phi_m(\beta)$ which identifies the subset of basins that are preferentially occupied at the given temperature.

Free energy expression, Eq. (3.2), encompasses the full range of equilibrium phase transitions, including the melting/freezing transition, and crystal polymorphic transitions, if any. However the expression is also useful for studying extensions into metastable phase regimes. If attention centers on the supercooled liquid down to the glass transition range, one requires that basins whose inherent structures show any substantial regions of crystalline order be projected out of consideration. Thus σ and f_v appearing in Eq. (3.2) would refer only to the amorphous subset of inherent structures and their basins. The variationally determined order parameter $\phi_m(\beta)$ then describes the normal and the supercooled liquid down to the glass transition range [9].

Beyond consideration of the free energy, separation of the inherent structure (σ) and vibration (f_v) aspects yields other nontrivial consequences. In the case of simple, Lennard–Jones-like systems computer simulation demonstrates that at constant volume the temperature dependence of short-range order resides almost exclusively in the amplitude of vibrational motion. After invoking steepest-descent mapping to remove all vestiges of vibrational deformation, the resulting collection of inherent structures exhibits strongly enhanced short-range order that is virtually temperature-independent. This is clear from the $\phi_m(\beta)$, from the pair correlation function [2,10], and from the distribution of void sizes [11]. The separation has also led to formulation of an inverse Lindemann criterion for the freezing of liquids, keyed to the rms vibrational displacements within amorphous-structure basins [6,12].

4. Hypercube model

The general properties listed in Section 2 for basin equivalence classes and their transition-state interconnections present a topology that qualitatively resembles that for the vertices and edges of a high-dimensional hypercube. The similarity has been noticed before [13]. This section presents a variant of the hypercube model that will be useful for discussing kinetic properties in Section 5.

In order that the hypercube have as many vertices as the condensed phase has distinguishable inherent structures [$\exp(\alpha N)$], the dimension D of the hypercube must be

$$D = \alpha N / \ln 2. \tag{4.1}$$

Without any significant loss of generality, it will be assumed that D is an even integer. Hypercube geometry implies that D is also the number of connections (possible transitions) from any vertex (basin equivalence class) to neighboring vertices (contiguous equivalence classes), thus showing the correct order in N.

For simplicity suppose that the 2^D hypercube vertices are located at the unit vector positions

$$\boldsymbol{\tau} \equiv D^{-1/2}(\pm 1, \pm 1, \ldots, \pm 1). \tag{4.2}$$

Edges connect pairs of vertices whose locations differ only by sign change of a single $\boldsymbol{\tau}$ component. Next, two of the $\boldsymbol{\tau}$'s are chosen to define a plane into which all $\boldsymbol{\tau}$'s will be projected. The two are:

$$\begin{aligned} &\boldsymbol{\tau}_x \equiv D^{-1/2}(1, 1, \ldots, 1), \\ &\boldsymbol{\tau}_y = D^{-1/2}(1, 1, \ldots, 1, \\ &\qquad\qquad -1, -1, \ldots, -1), \\ &\boldsymbol{\tau}_x \cdot \boldsymbol{\tau}_y = 0, \end{aligned} \tag{4.3}$$

where the first has all positive components, the second has $D/2$ positive components followed by $D/2$ negative components. The x, y position of any projected vertex,

$$x = \boldsymbol{\tau} \cdot \boldsymbol{\tau}_x, \qquad y = \boldsymbol{\tau} \cdot \boldsymbol{\tau}_y, \tag{4.4}$$

falls within the square defined by

$$|x + y| \le 1, \qquad |x - y| \le 1. \tag{4.5}$$

Many vertices can project onto the same location in the x, y plane; in the large D (i.e. large N) limit, their density in the square (4.5) is given by $\exp[Dw(x, y)]$, where [13]

$$\begin{aligned} w(x, y) = \ln 2 &- (1/4)[(1 + x + y) \\ &\times \ln(1 + x + y) \\ &+ (1 + x - y)\ln(1 + x - y) \\ &+ (1 - x + y)\ln(1 - x + y) \\ &+ (1 - x - y)\ln(1 - x - y)]. \end{aligned} \tag{4.6}$$

Experimental heat capacity measurements for various substances in both their crystalline and amorphous solid forms (glass states below T_g) suggest that vibrational degrees of freedom contribute roughly state-independent amounts to thermodynamic properties [14–17]. For this reason we can suppose that f_v is sufficiently close to constant across basin equivalence classes to disregard in the hypercube model. Specifically, changes of state are assumed to be driven principally by the interplay between structural entropy and structural interaction energy.

The potential energy values Φ_{is} at the inherent structures represented by the hypercube vertices can be expressed as follows:

$$\Phi_{is}(\boldsymbol{\tau}) = D\eta(\boldsymbol{\tau}) + \zeta(\boldsymbol{\tau}). \tag{4.7}$$

This separates Φ_{is} into an O(N) portion assumed to vary smoothly over the hypercube (η), from an O(1) portion that may vary in an irregular way from one vertex to its neighbors. In fact it will be assumed that η depends only on the distinguished coordinates x and y, which can be identified qualitatively as measuring the amount and the type of structural disorder present in the inherent structures.

Although $\zeta(\boldsymbol{\tau})$ plays an important role in kinetic properties (see Section 5), it does not influence thermodynamics. The hypercube model's $\phi_m(\beta)$ that identifies the preferred basin depth at temperature $T = (k_B\beta)^{-1}$ is determined by the following analog to Eq. (3.2) above:

$$\begin{aligned} \beta F_{hc}(\beta)/D &= \min_{(x,y)}\{\beta\eta(x, y) - w(x, y)\}, \\ \phi_m(\beta) &= (D/N)\eta[x_m(\beta), y_m(\beta)]. \end{aligned} \tag{4.8}$$

The indicated minimization is to be carried out over square (4.5), of course.

In order to be at all realistic, the "smooth" interaction function should lead to distinct "crystal" and "liquid" phases, and the latter should be amenable to metastable extension into the supercooled regime as explained in Section 3. The following simple choice fulfills these requirements:

$$\begin{aligned} \eta(x, y) &= x + y - (x - y + 0.2)^2 \\ &\quad + A(x - y + 0.2)^3, \\ A &= 0.4464285714, \end{aligned} \tag{4.9}$$

and is convenient for numerical examination. The absolute minimum of this function in the square occurs at the vertex $(-1, 0)$:

$$\eta(-1, 0) = -1.868571429, \tag{4.10}$$

and this should be identified as a "perfect crystal". A relative minimum occurs at another square vertex, $(0, -1)$,

$$\eta(0, -1) = \eta(-1, 0) + 0.2, \tag{4.11}$$

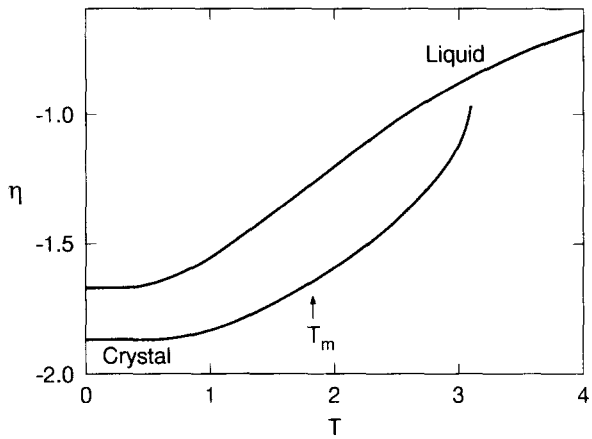

Fig. 1. Temperature variations of $\eta_m \equiv N\phi_m/D$ for crystal and liquid phases in the hypercube model.

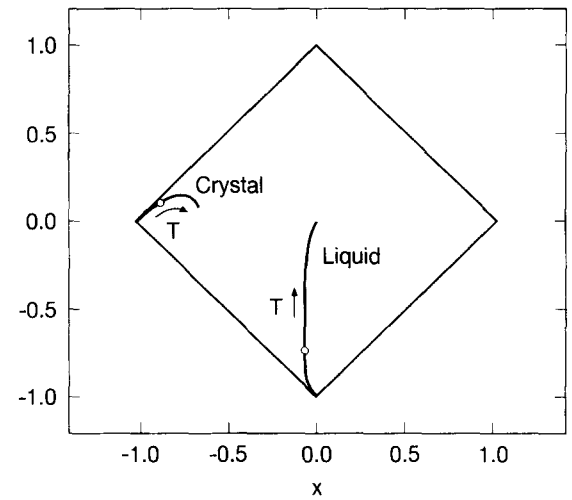

Fig. 2. Paths traced out in the fundamental (x, y)-plane square by the variationally determined $x_m(\beta)$, $y_m(\beta)$. Arrows indicate directions of increasing temperature, and open circles locate the melting/freezing transition.

and may be identified as a "fully structurally relaxed glass".

Numerical analysis reveals that $\phi_m(\beta)$ has two branches. They connect at absolute zero, respectively, to the absolute and relative minima indicated in Eqs. (4.10) and (4.11); consequently they can be identified as "crystal" and "liquid" branches. Fig. 1 indicates the temperature variation of $\eta_m(\beta) \equiv (N/D)\phi_m(\beta)$ for the two branches, and also shows the melting point

$$T_{\mathrm{mp}} = (k_B\beta_{\mathrm{mp}})^{-1} = 1.8311 \tag{4.12}$$

at which the two phases attain equal free energies. Notice that the crystal branch has a metastable extension beyond this melting temperature that finally terminates at a critical instability temperature

$$T_{\mathrm{c}} = (k_B\beta_{\mathrm{c}})^{-1} \simeq 3.09. \tag{4.13}$$

At this point the marginally metastable crystal must be viewed as highly defective, and its inherent structure potential energy has approached that of the liquid.

Fig. 2 indicates the paths traced out in the x, y plane by $x_m(\beta), y_m(\beta)$ for the two branches generated by the variational criterion, Eq. (4.8). Notice that these paths are well separated. Therefore the projection operation alluded to in Section 3 to avoid phase transitions and to enforce metastability is particularly simple for the present hypercube model. One needs only to cut the x, y square shown in Fig. 2 into two portions, one containing the crystal path, the other the liquid path. The respective subsets of hypercube vertices (inherent structures and their basins) then serve as the projected sets required for superheated crystal or supercooled liquid.

Configurational entropies of the crystal and liquid phases are equal to

$$S_{\mathrm{c}}/Nk_{\mathrm{B}} = (D/N)w(x_m, y_m). \tag{4.14}$$

The numerical calculations reveal that the supercooled liquid entropy lies above that of the crystal for all positive temperatures. This violates the concept of a positive "Kauzmann temperature" T_{K} at which equality is often presumed to obtain [9,18]. However the heat capacity of the supercooled liquid in the hypercube model significantly exceeds that of the crystal for a substantial temperature range below T_{mp}, and consequently the usual thermodynamic extrapolation to identify a $T_{\mathrm{K}} > 0$ can be misleading. Fig. 3 shows

$$\Delta w = w(\mathrm{liq}) - w(\mathrm{crys}), \tag{4.15}$$

proportional to the entropy difference, from the equilibrium freezing point down to $T = 0.60$, an hypothetical "glass transition temperature". Naive, but

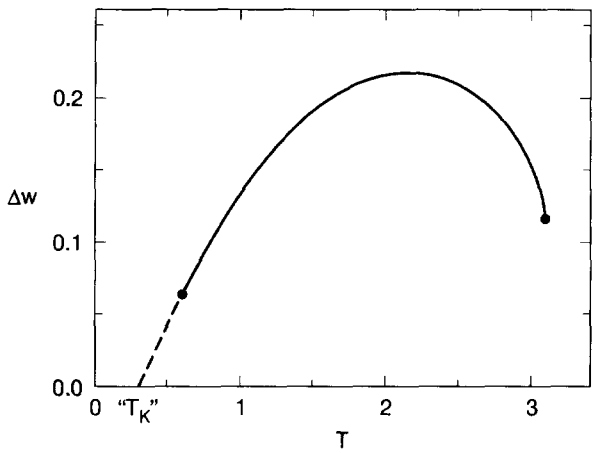

Fig. 3. Temperature variation of $\Delta w = w(\text{liq}) - w(\text{crys})$ from the melting point down to a "glass transition" at $T = 0.60$. Naive extrapolation (dotted curve) suggests the presence of an artifactual Kauzmann point at $T_K \simeq 0.30$.

seemingly reasonable, extrapolation to yet lower temperature suggests the presence of a Kauzmann point at

$$T_K \simeq 0.30. \tag{4.16}$$

In fact the correct curve bends smoothly back to encounter the horizontal axis only at absolute zero.

At the thermodynamic melting/freezing transition,

$$\Delta w(T_{mp}) = 0.21122. \tag{4.17}$$

For reference purposes it may be useful to make this correspond to the fusion entropy of a familiar real glass former. Chang and Bestul [15] have reported for *ortho*-terphenyl that

$$\Delta S = 52.196 \pm 0.02\,\text{JK}^{-1}\,\text{mol}^{-1} \tag{4.18}$$

(m.p. $\simeq 330$ K). Consistency between Eqs. (4.17) and (4.18) can be attained if

$$D/N \simeq 29.67, \tag{4.19}$$

or equivalently

$$\alpha \simeq 20.57. \tag{4.20}$$

Considering the asymmetry and internal-rotation flexibility of each *ortho*-terphenyl molecule, these estimates may not be unrealistically large.

5. Hypercube kinetics

Fig. 4 schematically illustrates a portion of the x, y plane onto which hypercube vertices have been projected. Those projected positions formally present a square lattice with possible dynamical transitions occurring only between nearest neighbors; these allowed transitions are indicated by solid lines in Fig. 4. In any transition, both x and y change by the small amount $\pm\Delta$,

$$\Delta = 2/D = 2\ln 2/\alpha N. \tag{5.1}$$

One must remember that many inherent structure equivalence classes, numbering $\exp[Dw(x, y)]$, project onto the same site in the x, y plane, but no pair of these are connected by a direct transition. Similarly, each solid line in Fig. 4 represents many

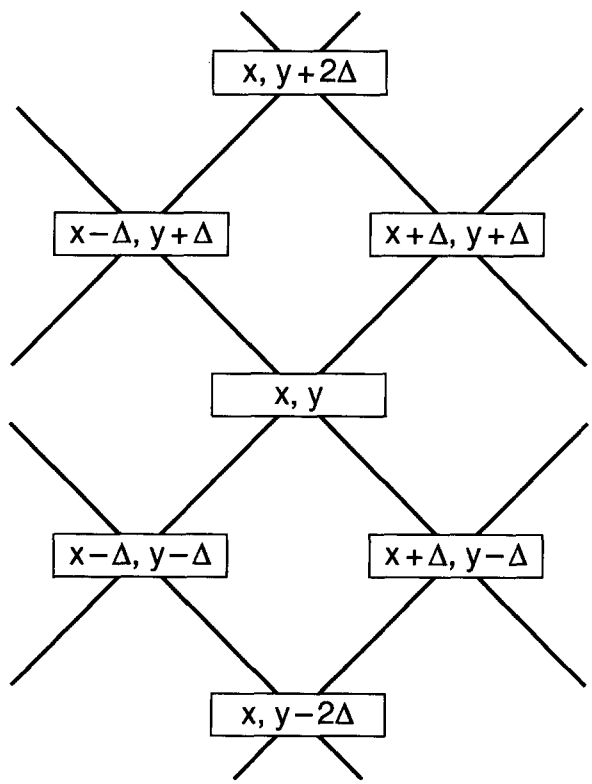

Fig. 4. Dynamical connections for the hypercube model as projected into the x, y plane. Boxed pairs indicate relative x, y values for the inherent structure equivalence classes, with $\Delta = 2/D$. Diagonal solid lines connecting neighbors represent allowed transitions.

transitions between pairs of inherent structure equivalence classes, but not all pairs that have projected onto neighboring sites can interconvert dynamically.

The extent of ruggedness of the potential energy landscape is at least partially conveyed by the function $\zeta(\tau)$ in Eq. (4.7). Experimental observations of kinetic rates displayed by real glass formers strongly indicates that its average amplitude and texture of ruggedness must vary with position as projected in the x, y plane. This is particularly evident in the starkly non-Arrhenius behavior of shear viscosity and of various other measures of structural relaxation for the so-called fragile glass formers [4,5]. It is also evident from the existence of stretched exponential (Kohlrausch–Williams–Watts) relaxation functions with temperature-dependent stretching exponents [19,20]. The weight of evidence requires $\zeta(\tau)$ to exhibit greater and greater amplitude of ruggedness upon approaching the low-temperature-glass region of the x, y plane, and to show a tendency toward organization into locally low-potential "craters" [6]. Low-temperature supercooled-liquid primary relaxation, the "α" process, is dominated by the need for the system to escape one of these craters by a coherent sequence of interbasin transitions ("β" processes), and to search a wide range in the configuration space to find an equally deep, or deeper, crater.

If ζ were simply a smooth function of x and y as postulated for η, then the time-dependent system probability in the x, y plane, $Q(x, y, t)$, can be shown to satisfy a Fokker–Planck equation:

$$\partial Q/\partial t = -\nabla \cdot [(\boldsymbol{\mu} \cdot \mathbf{F})Q] + \beta^{-1}\nabla \cdot (\boldsymbol{\mu} \cdot \nabla Q). \tag{5.2}$$

Here ∇ is the two-dimensional gradient in the x, y space, $\boldsymbol{\mu}$ a symmetric mobility tensor, and $\mathbf{F}$ is a thermodynamic mean force vector (the reader is referred to Ref. [13] for details). Now, with explicit inclusion of potential landscape ruggedness through incorporation of ζ spatial variations, Eq. (5.2) requires extension. The natural generalization that encompasses the temporal dispersion generated by potential ruggedness is a Fokker–Planck integrodifferential equation with nonlocality in time:

$$\partial Q/\partial t = \int_{-\infty}^{t} \{-\nabla \cdot [(\boldsymbol{\mu}(t-t') \cdot \mathbf{F})Q(t') + \beta^{-1}\nabla \cdot [\boldsymbol{\mu}(t-t') \cdot \nabla Q(t')]\}\, dt'. \tag{5.3}$$

A basic challenge is to relate the time-retarded mobility in this formulation to details of ζ, and specifically to show connections to temperature-dependent stretched exponential relaxation.

It should be mentioned in passing that Campbell et al. [21] have also investigated relaxation kinetics on hypercubes. Their specific model was simpler than that considered here, involving no explicit potential energy or temperature, but only random vertex dilution and uniform transition rates between surviving pairs of neighboring vertices. Stretched exponential relaxation was observed with stretching exponent that depended on the percolation probability for dilution.

One of the long-standing propositions concerning supercooled liquids was advanced by Adam and Gibbs [22], connecting mean structural relaxation times τ_{av} to configurational entropy S_c. Specifically, the Adam–Gibbs concept of independent "cooperatively rearranging regions" in the cold liquid leads to the relation:

$$\tau_{av}(T) \propto \exp[C/TS_c(T)], \tag{5.4}$$

where C is a positive constant. If a positive Kauzmann temperature T_K were to exist for the fully relaxed liquid, then Eq. (5.4) predicts that τ_{av} would strongly diverge at that point. The Adam–Gibbs relation seems to have had an unclear role in explaining experimental and simulational data, with reports both of success [23,24] and failure [25–27].

Quite apart from the fact that the present hypercube model does not support the existence of a $T_K > 0$, it also questions the universality of the Adam–Gibbs relation (5.4) on other grounds. Thermodynamic properties such as $S_c(T)$ depend *only* on the smooth background potential function η; kinetic transition rates and structural relaxation phenomena require specification of landscape ruggedness function ζ and the interbasin transition rates (dependent on transition state barrier heights, etc.). Consequently, the two sides of Eq. (5.4)

are logically disconnected at the level of mathematical modelling. If the Adam–Gibbs relation is to be put on a firm deductive basis for some class of materials, the underlying argument will have to establish that the special nature of the interactions involved force a linkage between η and ζ.

6. Discussion

The "rugged landscape" view of interactions in condensed phases, and its representation in terms of basins and inherent structures, provide helpful insights into a wide range of phenomena. But at the same time this approach generates many new questions. some of these may be simple to answer, while others are no doubt extremely challenging. This section atttempts to list some of the more significant open problems presented currently by the inherent structure representation.

From a mathematical viewpoint, the following issues require attention:

(1) Under constant volume or pressure conditions, is it possible to establish upper and lower bounds on α, the enumeration parameter for distinct Φ minima (Eq. (2.2))?

(2) In the asymptotic enumeration of Φ minima in free space, is Eq. (2.2) to be replaced by

$$\Omega \sim N! \exp(\text{const.} \times N^{P}) \quad p > 1, \tag{6.1}$$

a form suggested by simple fractal aggregation arguments?

(3) What are the occurrence probabilities for multiply connected basins with internal saddle points, and for transition states between permutationally equivalent basin pairs?

(4) What are the preferred geometries of inherent structures underlying critical fluids and dilute vapors?

(5) What is the high-temperature limiting behavior of the Lindemann ratio [6,12] for the constant-density fluid?

(6) What is the behavior of inherent structures in the mathematical limits of (a) short-range attractions, (b) smooth long-range interactions, (c) approach to hard spheres, and (d) large space dimension ($\gg 3$)?

Open problems possessing a more chemical orientation form a second list.

(7) Are thermally driven chemical equilibria in liquids, such as

$$H_2O \rightleftarrows H^+ + OH^-,$$

shifted by steepest descent mapping (SDM)?

(8) How does the number of basins vary along homologous series (e.g. normal alkanes)?

(9) How do inherent structures compare between pure optical isomers and their racemic mixtures?

(10) Does SDM always increase liquid–crystal order (nematic, cholesteric)?

(11) How do biopolymer solution inherent structures depend on primary squence, and on solvent composition?

(12) Are there materials or realistic models which demonstrably possess a true "ideal glass transition" at a positive Kauzmann temperature T_K?

(13) Does SDM preserve local neutrality and "second moment" conditions on electrolyte pair correlation functions [28]?

(14) How does SDM affect the diffuseness of liquid–liquid and liquid–vapor interfaces?

(15) How are interbasin transition states distributed (in height, etc.) for chemical reactions?

References

[1] F.H. Stillinger and T.A. Weber, Phys. Rev. A 25 (1982) 978.
[2] F.H. Stillinger and T.A. Weber, Science 225 (1984) 983.
[3] F.H. Stillinger, J. Chem. Phys. 89 (1988) 4180.
[4] C.A. Angell, in: Relaxations in Complex Systems, eds. K. Ngai and G.B. Wright (National Technical Information Service, US Dept. of Commerce, Springfield, VA, 1985) p. 1.
[5] C.A. Angell, Science 267 (1995) 1924.
[6] F.H. Stillinger, Science 267 (1995) 1935.
[7] W.A. Phillips, J. Low Temp. Phys. 7 (1972) 351.
[8] P.W. Anderson, B.J. Halperin and C.M. Varma, Philos. Mag. 25 (1972) 1.
[9] F.H. Stillinger, J. Chem. Phys. 88 (1988) 7818.
[10] F.H. Stillinger and T.A. Weber, J. Chem. Phys. 80 (1984) 4434.

[11] D.S. Corti, P.G. Debenedetti and F.H. Stillinger, to be published.
[12] R.A. LaViolette and F.H. Stillinger, J. Chem. Phys. 83 (1985) 4079.
[13] F.H. Stillinger, J. Phys. Chem. 88 (1984) 6494.
[14] S.S. Chang, J.A. Horman and A.B. Bestul, J. Res. Nat. Bur. Stds. A 71 (1967) 293.
[15] S.S. Chang and A.B. Bestul, J. Chem. Phys. 56 (1972) 503.
[16] R. Calemczuk, R. Lagnier and E. Bonjour, J. Non-Cryst. Solids 34 (1979) 149.
[17] S.S. Chang and A.B. Bestul, J. Chem. Thermodynamics 6 (1974) 325.
[18] W. Kauzmann, Chem. Rev. 43 (1948) 219.
[19] K.L. Ngai, Comments Solid State Phys. 9 (1979) 127, 141.
[20] R. Böhmer, K.L. Ngai, C.A. Angell and D.J. Plazek, J. Chem. Phys. 99 (1993) 4201.
[21] I.A. Campbell, J.-M. Flesselles, R. Jullien and R. Botet, Phys. Rev. B 37 (1988) 3825.
[22] G. Adam and J.H. Gibbs, J. Chem. Phys. 43 (1965) 139.
[23] C.A. Angell and D.L. Smith, J. Phys. Chem. 86 (1982) 3845.
[24] G.H. Fredrickson and S.A. Brawer, J. Chem. Phys. 84 (1986) 3351.
[25] J.H. Magill, J. Chem. Phys. 47 (1967) 2802.
[26] W.T. Laughlin and D.R. Uhlmann, J. Phys. Chem. 76 (1972) 2317.
[27] T.A. Weber, G.H. Fredrickson and F.H. Stillinger, Phys. Rev. B 34 (1986) 7641.
[28] F.H. Stillinger and R. Lovett, J. Chem. Phys. 49 (1968) 1991.